Advanced Rotor Aerodynamics Concepts with Application to Large Rotorcraft

Matthew W. Floros
Raytheon ITSS
Moffett Field, California

Wayne Johnson
Army/NASA Rotorcraft Division
NASA Ames Research Center
Moffett Field, California

Michael P. Scully
Aeroflightdynamics Directorate (AMRDEC)
US Army Aviation and Missile Command, Ames Research Center, Moffett Field, California

A study was conducted using the comprehensive analysis CAMRAD II to explore performance enhancements to large rotorcraft. The aircraft considered were a 125 foot diameter six-bladed rotor helicopter and an 85 foot diameter four-bladed rotor tilt rotor. The objectives were to reduce power required and increase maximum lift. The effects of improved airfoils and active controls were investigated. Airfoils with higher maximum lift and with reduced drag were investigated. Results showed a moderate improvement in the maximum lift capability for the helicopter and a large improvement for the tilt rotor. For the helicopter, 2/rev individual blade control resulted in modest power savings in cruise flight, which increased with control amplitude and forward speed. The optimum phase for the individual blade control was relatively insensitive to both amplitude and forward speed. The influences of active twist, increased chord, increments in airfoil properties, and tilt rotor tip extensions were also investigated.

Introduction

One of the challenges likely to face the rotorcraft industry in the future is designing a new generation of transport rotorcraft that are significantly larger than current models. As rotor size increases, the scaling issues become more severe and the fraction of gross weight required for rotor and rotor controls increases. As a result, large rotorcraft use high disk loading to reduce rotor size and weight. However, high disk loading impacts both performance (high induced power) and operational suitability (high downwash velocity). The technology challenge is to enable large, low disk-loading rotors with affordable weight fractions.

One or several enabling rotor technologies will likely be required to produce the performance gains and weight savings necessary for a cost-effective large rotorcraft. Such technologies must provide greater maximum thrust from a given blade area and reduce the power required to achieve a given level of thrust. These performance improvements must be attained for the same or less weight for a given blade and disk area. This will result in less rotor and rotor controls weight to attain a given maximum thrust capability.

The purpose of the current study was to examine possibilities for rotor aeromechanics performance improvements and gain understanding of how these blade element level technologies interact to produce integrated rotor performance. This understanding will be used to guide future research.

Approach

The approach taken in this investigation was to design large rotorcraft (both helicopter and tilt rotor versions) based on advanced technology goals, and determine the rotor performance for these designs. The U.S. Army Rotary Wing Vehicle (RWV) Technology Development Approach (TDA) goals for FY05 were used for all rotorcraft components. This established targets for rotor performance using advanced technology. The second phase was to examine what performance enhancements might be achieved using specific advanced rotor concepts.

The design mission profile for these rotorcraft was a 20-ton load, 500 km mission radius, on an "Army hot day" (4000' MSL and 95° F). The vertical takeoff requirement was Hover Out of Ground Effect (HOGE) at 95% of Maximum Rated Power (MRP) on an "Army hot day." The cargo compartment of these rotorcraft had to be the same as that of a C-130 transport, 10 x 9 x 40 feet. Advanced technology rotorcraft designs

1

1. REPORT DATE **2002**	2. REPORT TYPE	3. DATES COVERED **00-00-2002 to 00-00-2002**	
4. TITLE AND SUBTITLE **Advanced Rotor Aerodynamics Concepts with Application to Large Rotorcraft**		5a. CONTRACT NUMBER	
		5b. GRANT NUMBER	
		5c. PROGRAM ELEMENT NUMBER	
6. AUTHOR(S)		5d. PROJECT NUMBER	
		5e. TASK NUMBER	
		5f. WORK UNIT NUMBER	
7. PERFORMING ORGANIZATION NAME(S) AND ADDRESS(ES) **Army/NASA Rotorcraft Division,Army Aviation and Missile Command,Aeroflightdynamics Directorate (AMRDEC), Ames Research Center,Moffett Field,CA,94035**		8. PERFORMING ORGANIZATION REPORT NUMBER	
9. SPONSORING/MONITORING AGENCY NAME(S) AND ADDRESS(ES)		10. SPONSOR/MONITOR'S ACRONYM(S)	
		11. SPONSOR/MONITOR'S REPORT NUMBER(S)	
12. DISTRIBUTION/AVAILABILITY STATEMENT **Approved for public release; distribution unlimited**			
13. SUPPLEMENTARY NOTES **Presented at the American Helicopter Society Aerodynamics, Acoustics, and Test and Evaluation Technical Specialists Meeting, San Francisco, CA, January 23-25, 2002**			
14. ABSTRACT			
15. SUBJECT TERMS			

16. SECURITY CLASSIFICATION OF:			17. LIMITATION OF ABSTRACT	18. NUMBER OF PAGES	19a. NAME OF RESPONSIBLE PERSON
a. REPORT **unclassified**	b. ABSTRACT **unclassified**	c. THIS PAGE **unclassified**	**Same as Report (SAR)**	**14**	

were created to satisfy these requirements. The basic parameters of these designs are given in Table 1.

The rotorcraft design synthesis which produced the information for Table 1 was also used to calculate the rotor trim conditions. This trim included the effects of airframe (wing, fuselage, and empennage) aerodynamics and engine mass flow (jet thrust and momentum drag). The resulting rotor trim parameters are given in Table 2.

Versions of these designs were also created using baseline rotor technology. The dimensions and gross weights of these baseline versions remained the same as the advanced technology designs to avoid scaling effects. The engines were scaled up to retain the same hover capability with less efficient rotors. The greater weight and greater power required by these baseline technology rotors resulted in reduced payload (less than the 20-ton design requirement).

The baselines for RWV TDA rotor technology were RAH-66 for helicopters and MV-22 for tilt rotors. Baseline rotor technology means here the same airfoils, twist, and planform as RAH-66 and MV-22. Rotor size, disk loading, design blade loading, blade aspect ratio, number of blades and hub concept were design parameters used to select the designs for this application. Note that although the starting points for the designs were existing successful designs and design variables such as disk loading and radius were chosen for a specific mission, the baseline designs were not necessarily optimal.

Given these designs and the predicted gap between baseline technology and FY05 technology, the next step was to determine if the FY05 goals could be realized, and what rotor technologies were likely to be able to bridge the gap.

The design points for the helicopter and tilt rotor were based on typical modes of operation for the two vehicles. For the tilt rotor, hover performance, airplane mode performance (180-300 kts), and maximum helicopter mode lift at 80 kts were design points. For the helicopter, hover performance, cruise performance (100-180 kts), and maximum lift at 80 kts and 150 kts were examined. The target performance enhancements are given in Table 3.

Specifically, for this paper, an increase in blade loading (C_T/σ) of 0.0256 at maximum lift was desired for both the helicopter and the tilt rotor. A power reduction of 1000 Hp was desired for the helicopter, and reductions of 400 Hp and 200 Hp in hover and forward flight were objectives for the tilt rotor.

Description of Advanced Concepts

Several possibilities for increased aeromechanics performance were investigated, some purely conceptual, others more physically motivated. The advanced technologies included improved airfoils, active blade twist and individual blade control (IBC), increased blade chord, and tip extensions for tilt rotors.

Table 1: Helicopter and tilt rotor configurations

Property	Helicopter	Tilt Rotor
Gross Weight	121,000	129,600
Disk Loading (psf)	9.9	11.4
Empty Weight (%GW)	53.9%	60.2%
Fuel Weight (%GW)	11.8%	7.7%
Engine Power (shp)	2 x 11,960	2 x 12,640
Rotor Radius R (ft)	62.5	42.5
Geometric Solidity σ	0.1065	0.0752
Number of Blades N_B	6	4
Blade Twist θ_T (deg)	11	47.3
Precone β_P (deg)	0	2
Articulation	Hinged	Gimbaled
First Flap Natural Frequency		
Cyclic Mode (per rev)	1.07	1.02
Collective Mode (per rev)	1.07	1.07
Tip Speed V_T (ft/sec)	725	750 / 626

Table 2: Typical helicopter and tilt rotor trim conditions at 1 g

Parameter	Helicopter	Tilt Rotor
Airspeed (kt)	80	80
Rotor Thrust (%GW)	101.8%	58.7%
Tip Path Plane Incidence (deg)	-0.36	-5.33
Rotor Lift (%GW)	101.8%	58.4%
Rotor Propulsive Force (%GW)	0.64%	5.45%
Airspeed (kt)	150	240
Rotor Thrust (%GW)	100.4%	9.00%
Tip Path Plane Incidence (deg)	-2.47	-87.7
Rotor Lift (%GW)	100.3%	0.36%
Rotor Propulsive Force (%GW)	4.33%	8.99%
Airspeed (kt)	180	280
Rotor Thrust (%GW)	100.5%	10.54%
Tip Path Plane Incidence (deg)	-3.56	-89.2
Rotor Lift (%GW)	100.3%	0.15%
Rotor Propulsive Force (%GW)	6.24%	10.54%

Table 3: Target Rotor Performance Improvements

Performance Metric	Baseline	Improvement
Helicopter		
Hover, Rotor Figure of Merit	0.75	3%
Cruise (100-180 kt), Rotor L/D_e	6.3/9.2 @ 100 / 180 kts	9%
Max Blade Loading (C_T/σ) at 80 / 150 kts	0.16/0.15	16%
Tilt Rotor		
Hover, Rotor Figure of Merit	0.81	4%
Cruise (180-300 kt), Rotor Propulsive Efficiency	0.75	2%
Max Blade Loading (C_T/σ) at 80 kts	0.16	16%

Modern airfoils can be employed to increase performance of existing rotor designs in either of two ways. First, they can increase the maximum lift coefficient and hence C_T/σ available for the vehicle. Second, they can simply reduce rotor drag so that additional transmission, engine, and fuel weight can be saved, leaving more weight available for payload.

Current technology helicopter and tilt rotor airfoils were modified with increases in maximum lift and reductions in drag to produce improved theoretical airfoils. Note that the means for achieving these increases were not specifically addressed. If the changes in lift and drag were shown to improve the performance, the next step would be to produce the required airfoil characteristics. The airfoil improvements are divided into two categories. The first set are thought to be achievable strictly with modern airfoil design, not requiring active control such as circulation control or slots. The second set are increments in $C_{l_{max}}$ and C_d and were examined for purely academic purposes.

Active control methods were also analyzed. Several technologies were investigated to produce twist distributions around the rotor disk. The pitch at a blade section is given by collective, cyclic, pretwist, and any active twist that might be present,

$$\theta = \theta_0 + \theta_{1c}(\psi) + \theta_{1s}(\psi) + \theta_T(R) + \theta_A(?) \qquad (1)$$

Each method produces a different type of active twist θ_A as a function of R, ψ, or both.

Individual blade control (IBC) was analyzed by adding 2/rev root pitch, or $\theta_A(\psi)$ input to the blades and varying amplitude and phase. The 2/rev blade motion could potentially redistribute the lift around the rotor disk to produce an overall increase in lift or reduction in power. Because IBC inputs changed the root pitch, steady and 1/rev inputs are equivalent to swashplate motions and are therefore not relevant.

A second active control method was active blade twist. In the case of active twist, steady and 1/rev inputs can change the lift distribution. With steady state active twist (i.e. zero frequency or $\theta_A(R)$), a helicopter rotor can have different twist in hover and forward flight to improve the efficiency of both modes. Also, 1/rev and 2/rev twist ($\theta_A(R, \psi)$) were examined for the same reasons as 2/rev IBC.

For the tilt rotor, only steady state active twist was examined. With steady state twist, rather than having to compromise between hover efficiency and propeller mode efficiency, the active twist could allow the blades to be optimized for both. This would help reduce the negative trade-off that occurs with having fixed twist. Active twist might be produced by smart materials or a flap on the blade, but for this investigation, active twist was prescribed without regard for the mechanism that might produce it.

Although not an advanced concept, increased chord was examined as a way to increase maximum lift for both the helicopter and tilt rotor. The purpose was to simulate advances in blade structures which would allow a larger chord for the same rotor weight. Increased chord was modeled as a 20% increase in the chord without any corresponding increase in blade weight.

Tip extensions were also examined to increase the effective rotor diameter for hover performance in the tilt rotor. The extensions were assumed to be half of the tip chord and 11% of the nominal rotor radius.

Description of Rotor Models

The rotor performance was calculated using the comprehensive analysis CAMRAD II. The capability of CAMRAD II (Ref. 1) to accurately calculate rotor performance has been demonstrated for helicopters (Refs. 2 and 3) and for tilt rotors (Ref. 4). The rotor models were intended to be as basic as possible to isolate the effects of each advanced concept. The rotors featured rigid blades and rigid control systems and were configured as isolated rotors in a wind tunnel. For trim conditions, the rotor was trimmed to zero first harmonic flapping. The tilt rotor was modeled as a single rotor. The details of the helicopter and tilt rotor configurations are summarized in Table 1. The rotor trim conditions are given in Table 2.

The focus of the current work was performance calculations rather than loads or vibration, hence the periodic response was calculated with the harmonic balance method with only two harmonics. A free wake model was used to obtain more accurate performance.

A static stall model was used for maximum lift calculations. Although high thrust conditions are affected by dynamic stall, it was assumed that differences in lift between the baseline and advanced models will be similar to those predicted with a static stall model. Given the uncertainty and approximate nature of current dynamic stall models, this approach was thought to be reasonable for a preliminary study.

Simple models were desirable to reduce computer time and obtain equilibrium solutions at comparable trim conditions. This allowed for large numbers of parameters to be varied to gain an overall picture of what each concept could provide. More detailed analysis and optimization would have required a greater definition of the vehicle design and were clearly beyond the scope of this work.

Results

Many of the potential active control methodologies pertinent to tilt rotors are different than those for helicopters. Accordingly, the results are divided between the helicopter and tilt rotor. For the helicopter, 2/rev individual blade control was examined most extensively; for the tilt rotor, improved airfoils were explored in some detail.

Helicopter Results

Several technologies were investigated to improve helicopter performance. Based on the preliminary study, 2/rev IBC root pitch was found to be able to provide a reduction in rotor power for the helicopter. This was carried forward to try to understand what was causing the power benefit. Improved airfoils were also examined to determine if any significant gains could be made with modern airfoil design. Several additional parameters were also modified to show their effects on thrust and power. The parameters included planform twist, chord, and increments in airfoil lift and drag properties.

Individual Blade Control

For the initial study, a matrix of airspeeds, amplitudes, and phases of the IBC inputs was established. The airspeed was varied from 100-180 kts, the amplitude from 1-3 deg, and the phase was swept from 0-360 deg in 30 deg increments. Rotor thrust was trimmed to C_T/σ of 0.092 for an Army hot day. The power required for the higher airspeeds is shown in Figure 1. The quantity shown is the sum of profile and induced power, $P_i + P_o$.

One clear conclusion is that it is a lot easier to increase the rotor power required than it is to reduce it. Such a result is not surprising considering higher harmonics in the rotor inflow tend to increase induced power. To get a net reduction, more power has to be saved elsewhere.

Despite this, there are several encouraging observations from the results of the initial matrix. First, the power savings becomes greater with both IBC amplitude and forward speed for the three speeds shown. At low speeds (not shown) the individual blade control produced little benefit. The second observation is that the minimum power point occurs at about 150 deg phase for every case. That is a potential implementation benefit, as the phase may not have to be varied with flight condition. Because the power savings is greatest at high speed and larger IBC amplitude, the 180 knot case with 3 deg amplitude was investigated more closely.

The profile and induced power for this case are shown individually in Figure 2. The total power curve at the top of the figure is the same as that in Figure 1. It is evident from the bottom of the figure that the induced power is the source of the power reduction. The trend of the curve with phase follows that of the total power very closely. In contrast, although the trend of the profile power also follows the total power trend, the magnitude is greater at all phase angles. At the optimum phase of 150 deg, it is nearly the same as the baseline, but still slightly higher.

The next question to be answered is how the lift and power are being distributed to achieve a net power reduction. A useful way to gain understanding of how the distributions of lift and power are changing is to look at the entire rotor disk at once. Of interest is the change from the baseline, i.e. the difference between the case with IBC and the case without. It is difficult to see specific quantitative information on 3D plots, but they give a good qualitative view of the entire rotor disk. For comparison, two IBC phase angles are examined, 150 deg, where IBC is most beneficial, and 300 deg, where it is most detrimental.

The changes in lift for these two cases are shown in Figure 3. Before continuing, it is important to describe how the information is displayed in the 3-dimensional plots. The orientation is important as it is sometimes difficult to get a good perspective that doesn't obscure important information. The data is arranged so that the direction of flight is along the $+y$-axis and $+x$-axis points toward the advancing side. As an additional aid, a radial line at 0 deg azimuth is readily identifiable. Since the plots are shown as differences between the baseline and IBC cases, the location of the zero line, or no difference, is important. In each figure, the zero-line is the border between the light and dark regions, light representing an increase, dark a decrease.
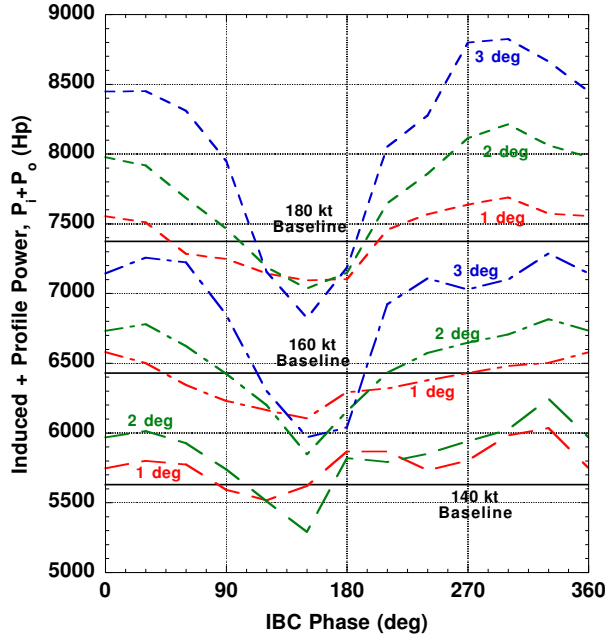
Figure 1: Effect of 2/rev individual blade control on helicopter power, C_T/σ=0.092, Army hot day
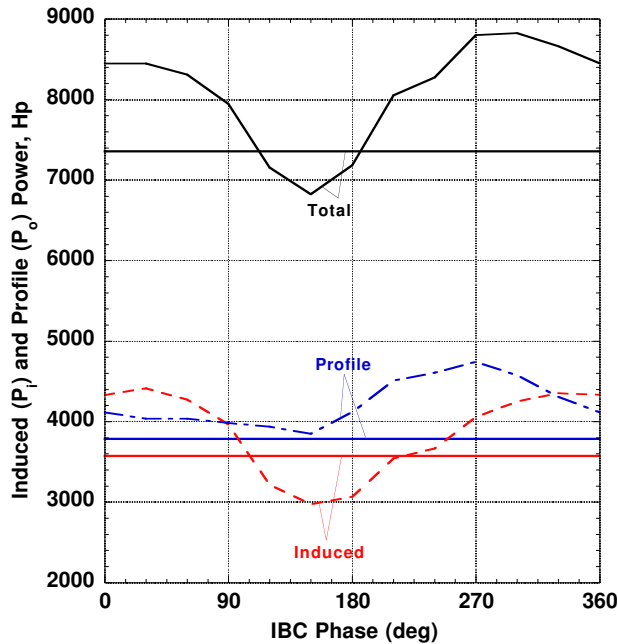

Figure 2: Profile and induced power for baseline helicopter and with 3 deg IBC, 180 kts, C_T/σ=0.092, Army hot day (Solid lines are baselines.)

The effect of the individual blade control is clear. The 150 deg phase IBC increases the lift in the first and third quadrants and decreases in the second. This is consistent with the peaks in 2/rev pitch occurring at 75 deg and 255 deg. There is also a lift decrease along the back of the rotor disk. The 300 deg phase IBC increases lift in the second and fourth quadrants, consistent with peaks in 2/rev pitch at 150 and 330 deg.

Note that for this comparison, the total thrust is unchanged with the individual blade control so any local thrust increase must be balanced by a decrease elsewhere on the disk. The rotor is trimmed, so the rolling and pitching moments with and without the individual blade control are also the same. Contrasting the two plots, the 150 deg plot shows more drastic changes in lift on the advancing side, where the retreating side is comparatively flatter. For the 300 deg case, there are significant changes in the lift distribution on both the advancing and retreating sides.

The induced power is shown in Figure 4. The general trend is that the induced power is transferred toward the blade tip on the front of the rotor disk, and shifted more inboard on the back of the disk and on the advancing side. In the front of the rotor disk, where the induced power is transferred to the tip, the power is increased at all radial stations (although only slightly inboard), thus the net effect is more induced power in that region.

For the case with 2/rev IBC at 300 deg phase, the induced power change follows the lift change closely. In this case, the moderate and large power increases in the second and fourth quadrants overwhelm the modest decreases in the first and third quadrants.

Figure 5 shows the profile and induced power integrated radially around the azimuth. From Figure 2, there is little change in the profile power between the case with IBC at 150 deg and the baseline. This is supported in Figure 5, where the two curves are nearly the same. The induced power, on the other hand, shows some significant differences. In the front of the disk and third quadrant, where power was transferred toward the tip, the induced power is higher for the IBC case. Over the remainder of the disk it is lower, particularly over the back of the disk and on the advancing side, consistent with the 3-D distributions in Figure 4. It is evident that the induced power change is dominating the total power change in Figure 4. Looking at Figures 4 and 5 together, the power is generally reduced where the lift is shifted inboard, and increased where it is shifted outboard.

A similar matrix of test cases was also calculated for 2/rev active blade twist. To simulate active twist, the rotor blade was given a large uniform torsional stiffness and an artificial twisting moment was applied to the tip with sufficient magnitude to obtain 1 or 2 deg of twist at the blade tip. This isolated the effect of the active twist from elastic blade torsion dynamics. Flap and lag remained rigid as in the other cases.
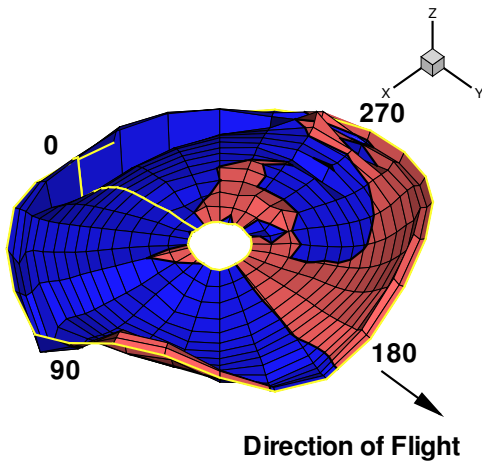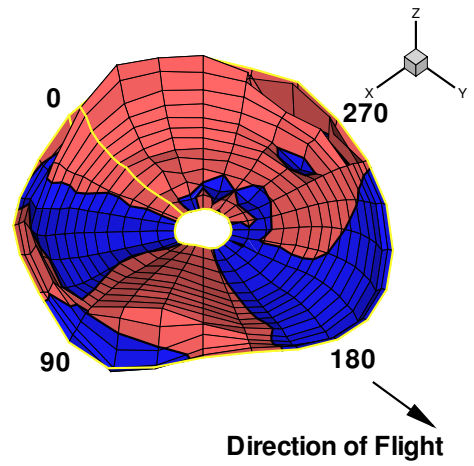
5
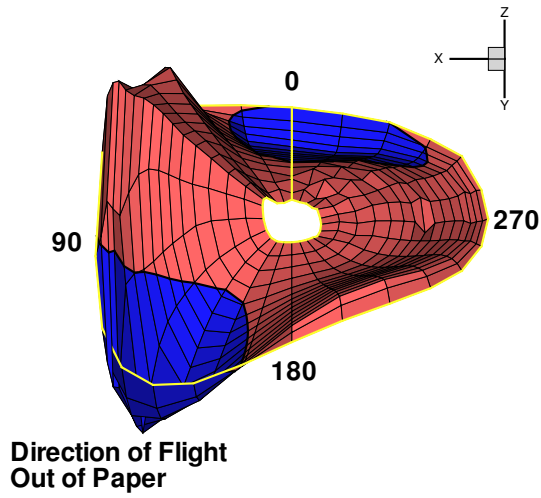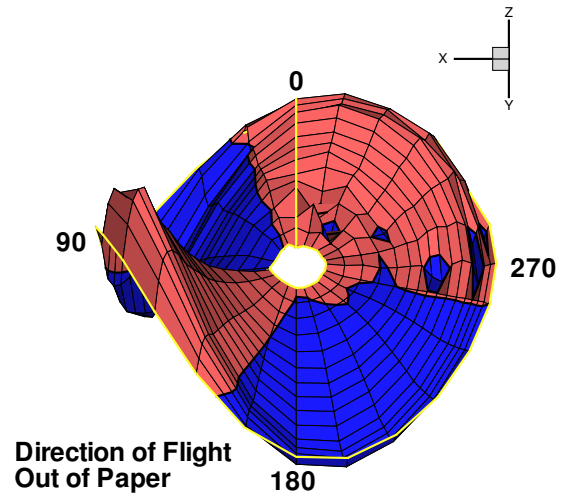
Figure 3: Rotor thrust distribution on a helicopter with 3 deg IBC, at 150 and 300 deg phase, 180 kts, C_T/σ=0.092, Army hot day. Difference between baseline and with IBC; light area is increase, dark area reduction

Figure 4: Rotor induced power distribution on a helicopter with 3 deg IBC, at 150 and 300 deg phase, 180 kts, C_T/σ=0.092, Army hot day. Difference between baseline and with IBC; light area is increase, dark area reduction

The variation of power (profile and induced power only) with amplitude and phase is shown in Figure 6. The trends have similarities and differences from those for IBC root pitch (Figure 1). The phase for the largest power reduction is around 150 deg with an approximately sinusoidal shape, similar to the trend with root pitch. Conversely, the magnitude of the power reduction was not as large as with root pitch and was about the same for 1 and 3 degrees amplitude in the higher speed cases. For these reasons, 2/rev active twist was not pursued further.

Improved Airfoils

Improved airfoils were also examined for performance enhancements. The goal of the improved airfoils was to increase the maximum lift at a given power. Although this would also reduce power at constant thrust, the increased thrust was the focus.

To generate an improved airfoil set, the drag of the baseline airfoils was modified. The improved blade was comprised of four airfoils derived from current technology helicopter airfoils. The procedure was to extend the drag rise of the existing airfoils to higher angles of attack. For each baseline airfoil, a stretching factor distribution was defined as a function of Mach number, $\Delta\alpha(M)$, and the drag rise was extended by that amount,

$$C_{d_{imp}}(\alpha) = C_{d_{base}}(\alpha - \Delta\alpha(M)) \qquad (2)$$

For example, a stretching factor of $\Delta\alpha = 7$ means that the improved airfoil drag at 10 degrees is set to the drag of the baseline at 3 degrees. Between Mach numbers of 0 and 0.3, the stretching factor was held constant. The stretching factor was applied from $+\Delta\alpha$ to 30 degrees angle of attack on the assumption that the minimum drag occurred at $\alpha = 0$ on the baseline airfoils. Angles from $0 \leq \alpha < \Delta\alpha$ were left unchanged, otherwise drag at small positive α might be replaced by higher drag from a negative α. The result is a stretching of the drag bucket from zero rather then a pure shift. Above $\alpha = 30$ deg, accurate airfoil data is normally not available.

The stretching factor distributions at the four spanwise stations are shown in Figure 7. For these airfoils, the drag at low and moderate Mach numbers was improved at the expense of drag at high Mach numbers. Figure 8 shows the 50% airfoil at two Mach numbers as an example. For $M = 0.3$, the drag is shifted 2 deg to the right; for $M = 0.6$, the drag is shifted about a degree to the left.

Although Mach numbers of 0.8 or higher can be found on the advancing tip in high speed flight, in such cases the airfoil is normally at a negative angle of attack. Therefore, low drag at positive angles of attack for high Mach numbers can be less important for normal cruise. Using four airfoils along the span
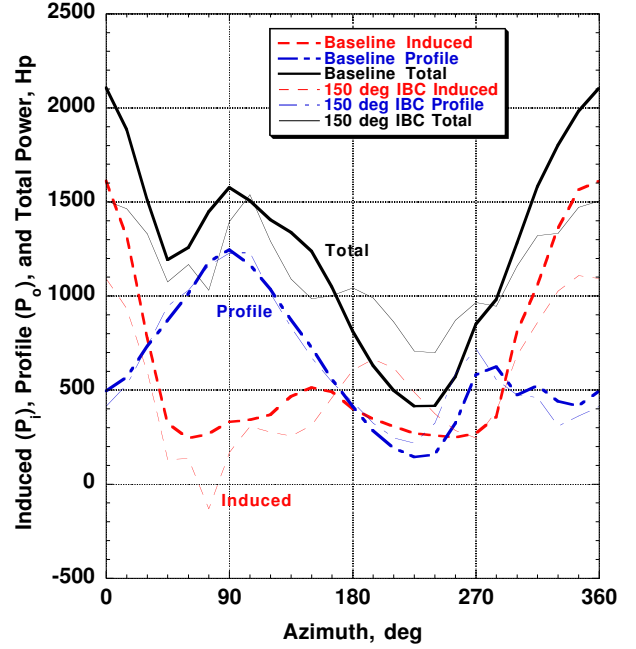

Figure 5: Profile and induced power on a helicopter with 3 deg IBC, 180 kts, C_T/σ=0.092, Army hot day
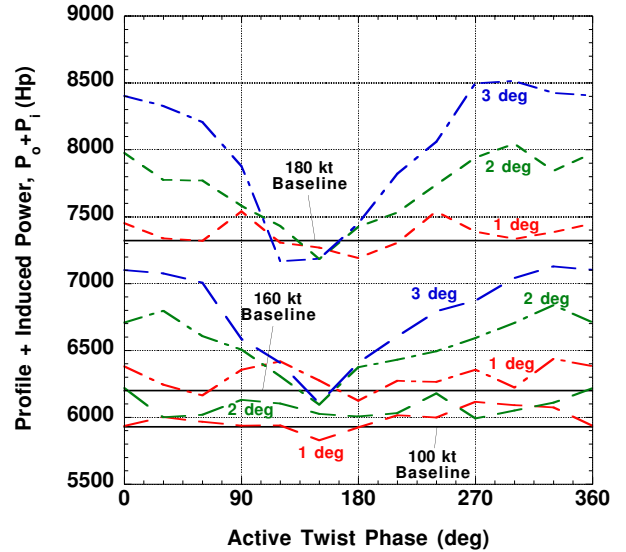

Figure 6: Power vs. active twist phase for a helicopter, C_T/σ= 0.092, Army hot day
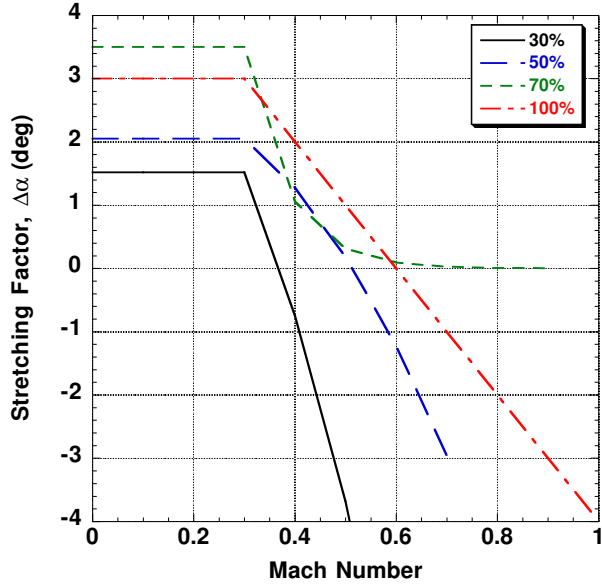
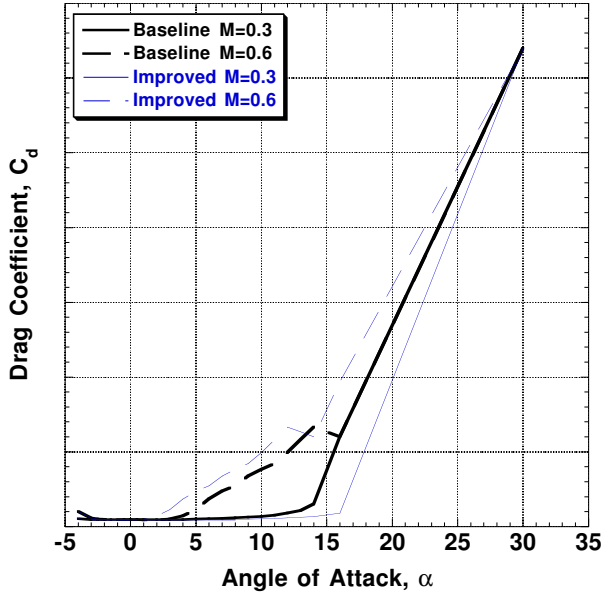Figure 7: Drag stretching factors for helicopter airfoils

Figure 8: Baseline and improved airfoil drag distributions for 50% helicopter airfoil

means that each airfoil section can be matched with the expected Mach number range it will encounter.

The maximum lift available from the rotor was calculated by sweeping the collective pitch and trimming to zero first harmonic flapping. Thrust and power results for 80 and 150 kts using the baseline and improved airfoils are shown in Figure 9. Looking horizontally from the baseline to the improved, a gain of about 0.004 in maximum C_T/σ at the same power is realized for both the high speed and low speed cases. Perhaps more important, looking vertically, at a given C_T/σ, there is a significant power reduction, up to several thousand horsepower. This shows that the combination of both improved and a greater number of airfoils along the span can potentially be beneficial.

Additional Planform and Airfoil Modifications

Several additional parameters were assessed and were found to have potential benefits. Zero-frequency twist, large pretwist (up to 19 deg), increased chord, and increased $C_{l_{max}}$ were found to improve the performance and maximum lift of the helicopter.

Calculations showed that zero frequency active twist ($\theta_A = \theta_A(R)$ only in equation 1) could have a significant benefit on hover power. A parametric sweep of twist is shown in Figure 10. Introducing an additional -8 deg twist reduces the power the most, by nearly 1800 Hp, almost doubling the 1000 Hp goal. Higher twist does not reduce the power as much as the -8 deg case, but continues to meet the reduction goal. If implemented, the twist could be provided by active control to reduce hover power and then turned off or used for some other purpose in forward flight.

Figures 11 and 12 show power required in hover and forward flight with increased chord and increments in $C_{l_{max}}$ and C_d. Note that the curves are plotted against the nominal solidity, as the real solidity increases with chord. Increased chord is intended to increase maximum lift and requires more power for a fixed thrust in both hover and forward flight. Conversely, increasing $C_{l_{max}}$ produces a small benefit in both hover and forward flight. Decreasing C_d saves slightly more hover power than increasing $C_{l_{max}}$.

The increments make more substantial differences in forward flight. The C_d decrement that made only a slight difference in hover power makes a more significant difference in forward flight. Figure 12 shows that the small decrement in C_d saves as much as 500 Hp in moderate to high speed flight. The $C_{l_{max}}$ increment is only a slight improvement over the baseline, and the increased chord results in more power required.

Large pretwist (θ_T in equation 1) also improves performance, but typically has a negative impact on vibration and loads in forward flight. If these issues could be solved, perhaps with a
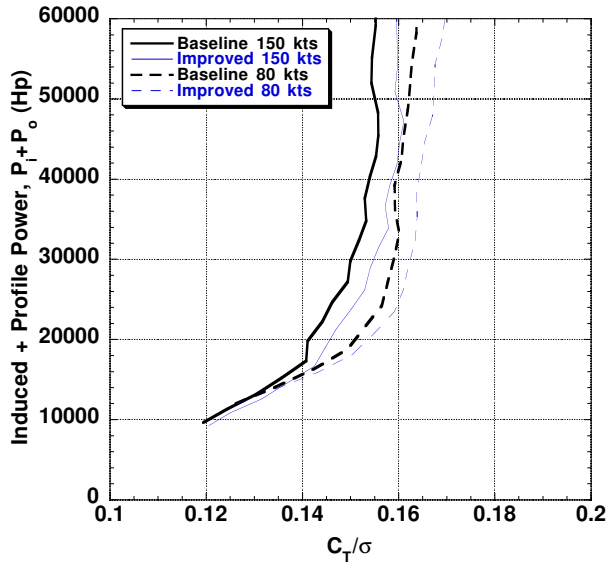
Figure 9: Power vs. Thrust for helicopter with baseline and improved airfoils at 80 and 150 kts, Army hot day
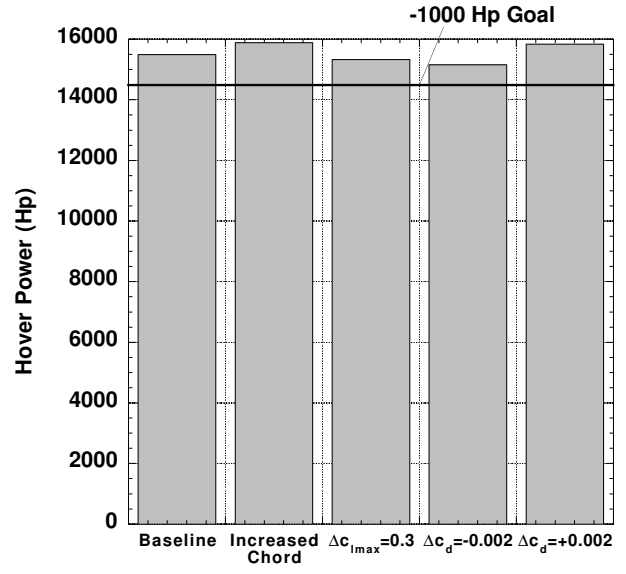

Figure 11: Hover power with increased chord and increments in airfoil properties, C_T/σ=0.092, Army hot day
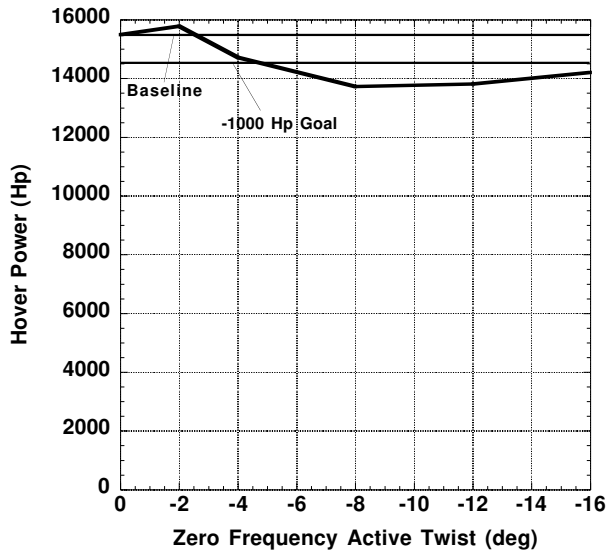

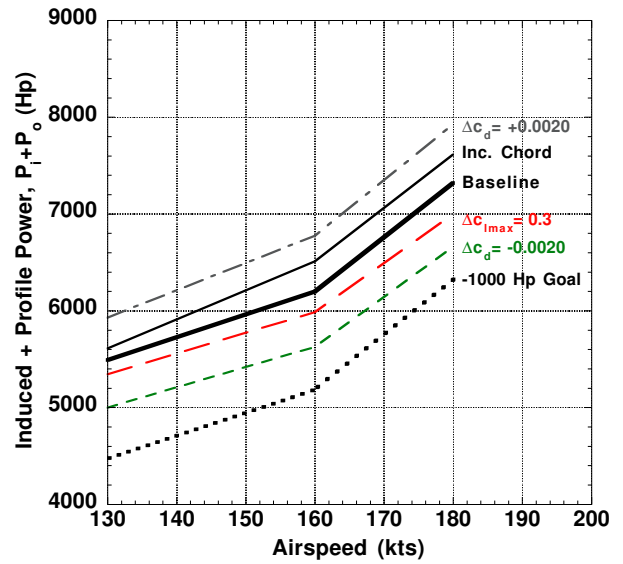Figure 10: Hover power with varying twist, C_T/σ=0.092, Army hot day

Figure 12: Induced and Profile power with increased chord and increments in airfoil properties, C_T/σ=0.092, Army hot day

9

different advanced technology, highly twisted blades are possible. When the increments in the airfoil properties are combined with large pretwist, the power savings is additive in hover. In Figure 13, the -19 deg twist still meets the 1000 Hp reduction goal in hover, but can be improved further with either the increased $C_{l_{max}}$ or decreased C_d.

In forward flight (Figure 14), the highly twisted blades consume more power than the baseline blades as speed increases. As with the baseline twist, the decrement to C_d makes the most significant difference. The power reduction for the modifications in both $C_{l_{max}}$ and C_d is larger at lower speed and then vanishes at very high speed.

Maximum lift could also be augmented by these technologies. The effects of increased chord and incremented $C_{l_{max}}$ are shown in Figure 15. As the rotor becomes deeply stalled, the maximum lift increase approaches $\Delta C_T/\sigma$ of 0.02 for both technologies. This is not quite the desired 0.0256 increment, but it is close. At lower power levels, the additional thrust tapers off to about 0.01 at 150 kts and nearly zero at 80 kts.

Increased twist, shown in Figure 16 adds to the benefit of increased $C_{l_{max}}$. By itself, the large twist increases maximum lift by about 0.01, but when combined with the $C_{l_{max}}$ increment, the total increase is on the order of the 0.0256 goal. As discussed previously, however, such large blade twist would likely require a separate treatment of vibration and loads.

Tilt Rotor Results

Many of the same technologies which were examined for the helicopter configuration were also assessed for the tilt rotor configuration. Although individual blade control was not addressed, improved airfoils, planform parameters, and airfoil increments were investigated. For the tilt rotor, the planform changes were increased chord and tip extensions. The airfoil lift and drag increments were similar to those applied to the helicopter airfoils.

Improved Airfoils

The effects of improved airfoils were also assessed on the tilt rotor. The goal was to increase the maximum lift at a given power. As in the helicopter case, the drag of the airfoils was reduced using $\Delta\alpha(M)$ stretching factors. The drag modifications alone did not significantly change the maximum lift capability.

Therefore, the maximum lift coefficient $C_{l_{max}}$ was also modified to simulate expected advances in airfoil design for tilt rotors. The maximum lift coefficient was increased by 0.3 at low Mach numbers, and tapered linearly to 0.05 from $0.3 < M < 0.8$, and held constant at 0.05 for Mach numbers above 0.8 (see Figure 17).
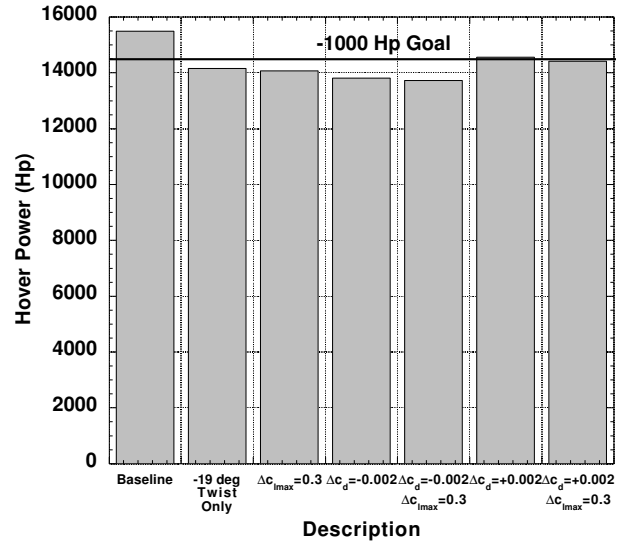

Figure 13: Hover power with large twist and increments in airfoil properties, C_T/σ=0.092, Army hot day (all except baseline have -19 deg twist)
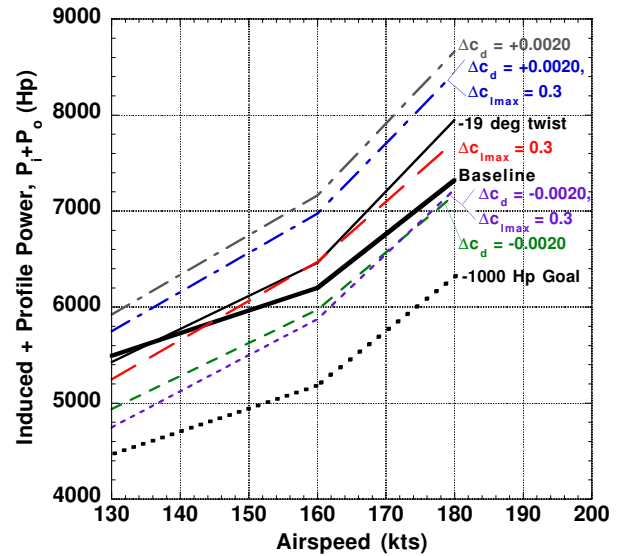

Figure 14: Induced and Profile power with large twist and increments in airfoil properties, C_T/σ=0.092, Army hot day (all except baseline have -19 deg twist)
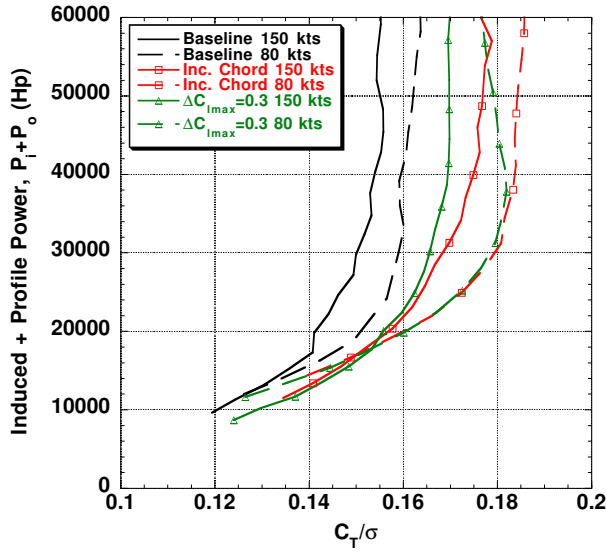
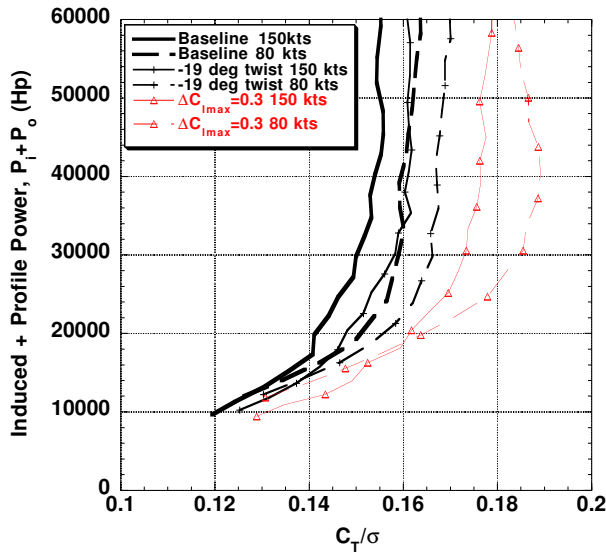Figure 15: Maximum lift with increased chord and increment in $C_{l_{max}}$, Army hot day

Figure 16: Maximum lift with large twist and increment in $C_{l_{max}}$, Army hot day (all except baseline have -19 deg twist)

The maximum lift at 80 kts with the baseline and improved airfoils is shown in Figure 18. Looking horizontally between the two curves, it can be seen that the maximum C_T/σ has been increased from about 0.16 to 0.18 at the same power, nearly the amount desired.

The logical question is then, where does the lift comes from? To illustrate, results are presented at constant power. The rotor with the baseline airfoils is at 12 deg collective; the rotor with improved airfoils is at 13 deg collective. A plot of the difference in thrust is shown in Figure 19. Although the rotor is generating additional lift over most of the disk, the dominant areas are about 75% span on the retreating half of the disk and the advancing side. There is a significant dip in thrust near the tip at approximately 60 deg. This negative region is balanced by increased thrust both before and after it.

The power distribution is shown in Figure 20. For this case, the thrust has increased over the baseline, but the power is constant, so Figure 20 shows only a shifting of power around the rotor disk. The predominant trend is for power to be moved toward the blade tip, which occurs for about half of the rotor azimuth. This shift is more pronounced on the retreating side, where the outer 15% span has increased power and the power is reduced at around 75% span. For the remaining quarter of the disk on the advancing side, the power shift is not as dramatic, and the power is shifted inboard rather than outboard. The combination of Figures 19 and 20 suggests that the additional load-carrying capability on the retreating side reduces negative lift (and thus power) on the advancing tip.

Additional Planform and Airfoil Modifications

Additional parameter changes were examined for the tilt rotor to obtain power reductions in hover and forward flight. Zero-frequency active twist, increased chord, tip extensions, and an increase of 0.3 in airfoil $C_{l_{max}}$ were investigated. The latter is not as realistic as the increase in the previous discussion, where the increment to $C_{l_{max}}$ decreased with Mach number, but was tested to see if it would provide any additional benefit.

As with the helicopter, zero-frequency active twist was found to improve the performance of the tilt rotor. Unlike the helicopter, however, the tilt rotor blades are highly twisted and hover performance improves when the rotor is *un*-twisted. Figure 21 shows the power change from an additional -4 deg to +4 deg twist (reducing the negative twist). By untwisting the blades 4 deg, 220 Hp can be saved, or about half of the 400 Hp goal.

In high speed forward flight, the rotor is in propeller mode. Propeller mode efficiency is increased when the blades are twisted more than a conventional tilt rotor. The total power for the rotor in cruise is shown in Figure 22. With -4 deg of active twist, the power is decreased by about 200 Hp, meeting the
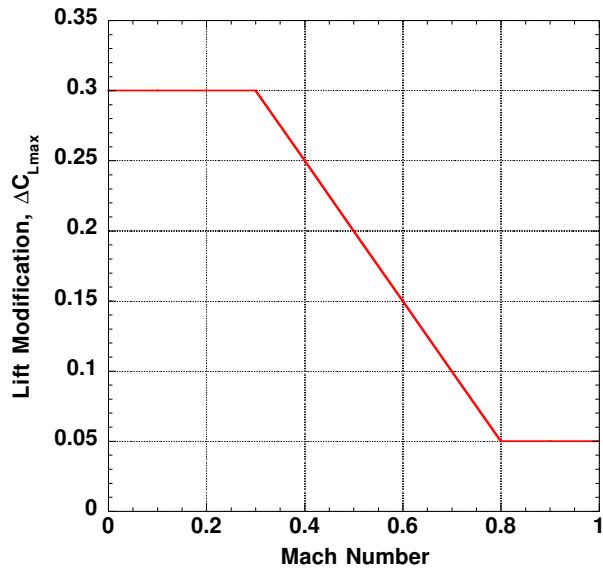
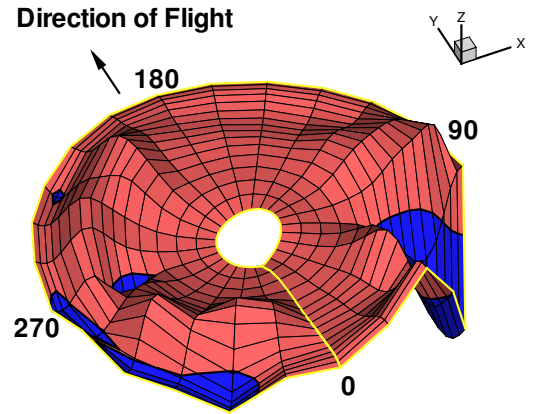Figure 17: Mach-varying lift correction for tilt rotor airfoils

Figure 19: Thrust increment of improved airfoils over baseline for tilt rotor in helicopter mode at 80 kts, Army hot day
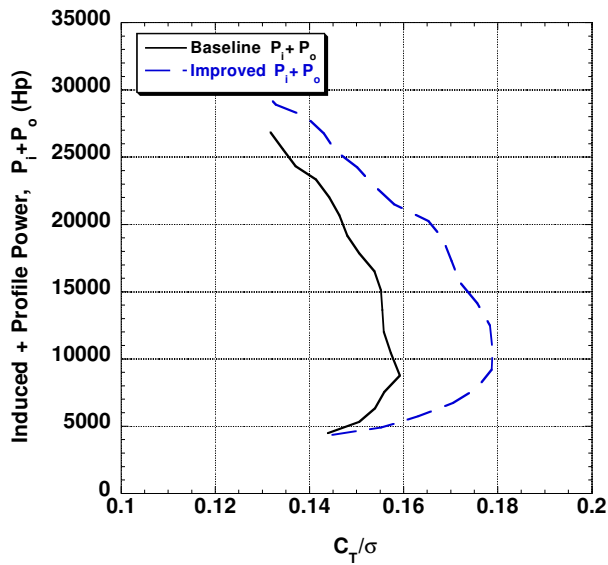

Figure 18: Maximum lift for tilt rotor in helicopter mode with baseline and improved airfoils at 80 kts, Army hot day
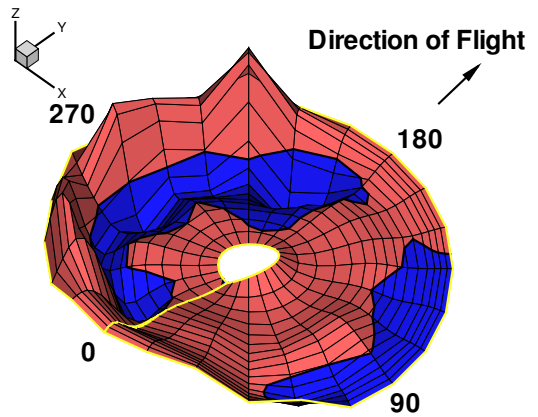

Figure 20: Power ($P_i + P_o$) increment of improved airfoils over baseline for a tilt rotor in helicopter mode at 80 kts, Army hot day

power objective for forward flight. Figures 21 and 22 together show that active twist can reduce the tradeoff between hover and cruise performance; power can be saved in both modes.

Hover power with tip extensions, increased chord, and increased $C_{l_{max}}$ is shown in Figure 23. The tip extension is the only parameter which meets the 400 Hp goal; in fact it more than triples it with more than a 1200 Hp reduction. The increased $C_{l_{max}}$ almost meets the goal. The increased chord, intended for maximum lift, requires more power in hover due to additional skin friction drag.

The advantage of increased chord is clear in the maximum lift, shown in Figure 24. Note that the curves are plotted against the nominal solidity, as the real solidity increases with both the tip extensions and increased chord. All three of the parameters do nearly as well for maximum lift, and are slightly better than the improved airfoil modification shown in Figure 18. The increased chord and $C_{l_{max}}$ increment meet the goal of a 0.0256 increase in C_T/σ while the tip extension is a little less. Because of the improvement in both maximum lift and hover power, the tip extension appears to be the most promising of the three options.

Conclusions

A parametric investigation of advanced technologies for a large helicopter and tilt rotor was conducted using the comprehensive analysis CAMRAD II. Several of the technology options were able to meet the reduced power and increased thrust goals. 2/rev individual blade control and improved tilt rotor airfoils were examined in detail. Additional planform and airfoil parameters were analyzed for both the helicopter and tilt rotor. Based on the test conditions in this study, the following conclusions can be made.

Helicopter:

1. 2/rev IBC root pitch was able to reduce helicopter power at high speed by up to 550 Hp, or about 7.5%. Power reductions correlated with lift being shifted inboard and away from the back of the rotor disk.

2. 2/rev IBC root pitch generally increased in effectiveness with increasing amplitude and forward speed.

3. An increment of -8 deg twist produced a significant power reduction in hover compared to the baseline.

4. Increments in $C_{l_{max}}$ and C_d could reduce power in hover and forward flight. Generally, -19 deg twist improved hover performance further but eroded performance gains at higher speed.

5. Increased $C_{l_{max}}$ and increased chord were able to produce a $\Delta C_T/\sigma$ of about 0.02, which was increased to about 0.025 with large pretwist.
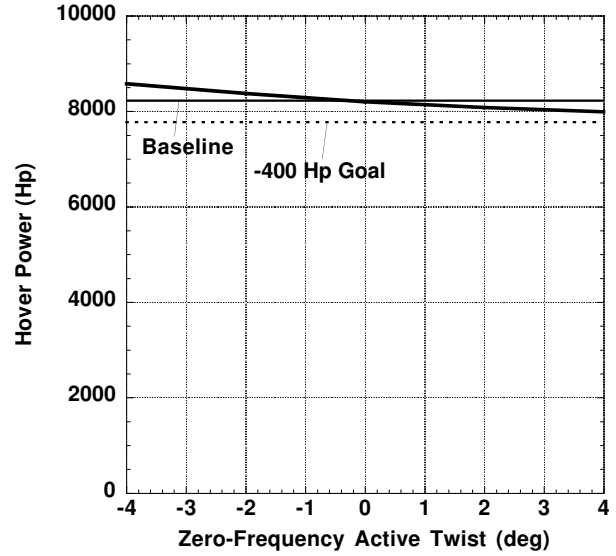

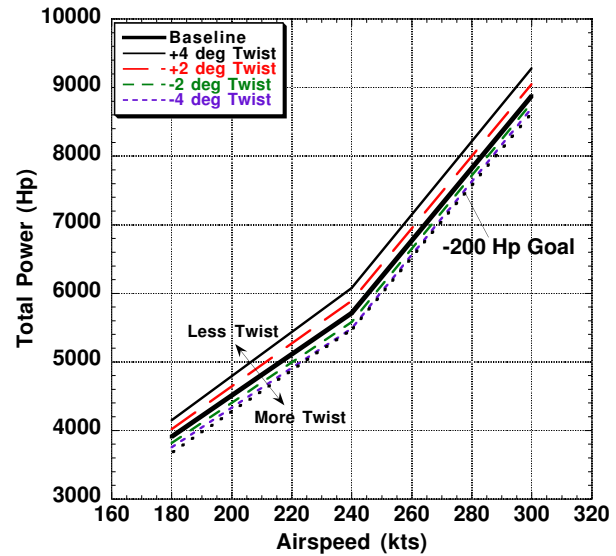Figure 21: Hover power for a tilt rotor with zero-frequency twist, Army hot day

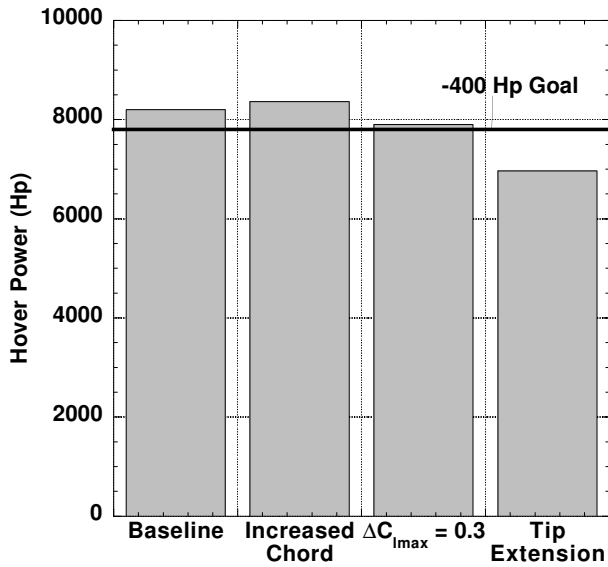Figure 22: Total cruise power for a tilt rotor with zero-frequency twist, Army hot day

13

Figure 23: Hover power for a tilt rotor with tip extensions, increased chord, and increased $C_{l_{max}}$, Army hot day
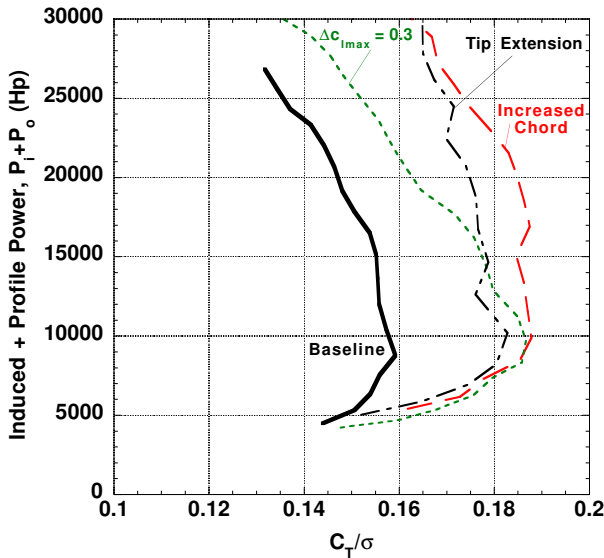

Figure 24: Induced and profile power for a tilt rotor in helicopter mode with tip extensions, increased chord, and increased $C_{l_{max}}$, 80 kts, Army hot day

Tilt Rotor:

1. Improved airfoils increased maximum lift by $\Delta C_T/\sigma$ of about 0.02. Lift was increased over nearly all of the disk, with concentrations at about 75% span on the retreating side and in the outboard advancing region. Power was transferred outboard on the retreating side and inboard on the advancing side.

2. Active twist was able to reduce the power by about 200 Hp in both hover and forward flight by untwisting the rotor in hover and increasing the twist in forward flight.

3. Tip extensions provided a significant reduction in hover power and maximum lift.

4. Increased chord improved maximum lift further but degraded hover performance.

References

[1] Johnson, Wayne, "Technology Drivers in the Development of CAMRAD II," *Proceedings of the American Helicopter Society Aeromechanics Specialists Conference*, San Francisco, CA, January 1994.

[2] Johnson, Wayne, "Rotorcraft Aeromechanics Applications of a Comprehensive Analysis," *Presented at Heli Japan 98: AHS International Meeting on Advanced Rotorcraft Technology and Disaster Relief*, Japan, April 1998.

[3] Yeo, Hyeonsoo, Bousman, William G., and Johnson, Wayne, "Performance Analysis of a Utility Helicopter with Standard and Advanced Rotors," *Proceedings of the American Helicopter Society Aerodynamics, Acoustics, and Test and Evaluation Specialist Conference*, San Francisco, CA, January 2001.

[4] Johnson, Wayne, "Calculation of Tilt Rotor Aeroacoustic Model (TRAM DNW) Performance, Airloads, and Structural Loads," *Proceedings of the American Helicopter Society Aeromechanics Specialists Conference*, Atlanta, GA, November 2000.